

# Convex Shape Prior for Multi-object Segmentation Using a Single Level Set Function

Shousheng Luo

Beijing Computational Science Research Center  
Building 9, East Zone, ZPark II,  
Haidian District, Beijing, China

sluo1983@csrc.ac.cn

Xue-Cheng Tai

Department of Mathematics  
Hong Kong Baptist University  
Kowloon Tong, Hong Kong

xuechengtai@hkbu.edu.hk

Limei Huo

School of Mathematics and  
Statistics, Henan University  
Kaifeng, China.

limei.huo@qq.com

Yang Wang

Department of Mathematics  
Hong Kong University of Science  
and Technology,  
Clear Water Bay, Hong Kong

yangwang@ust.hk

Roland Glowinski

Department of Mathematics  
University of Houston,  
Houston, TX 77204, USA

roland@math.uh.edu

## Abstract

*Many objects in real world have convex shapes. It is a difficult task to have representations for convex shapes with good and fast numerical solutions. This paper proposes a method to incorporate convex shape prior for multi-object segmentation using level set method. The relationship between the convexity of the segmented objects and the signed distance function corresponding to their union is analyzed theoretically. This result is combined with Gaussian mixture method for the multiple objects segmentation with convexity shape prior. Alternating direction method of multiplier (ADMM) is adopted to solve the proposed model. Special boundary conditions are also imposed to obtain efficient algorithms for 4th order partial differential equations in one step of ADMM algorithm. In addition, our method only needs one level set function regardless of the number of objects. So the increase in the number of objects does not result in the increase of model and algorithm complexity. Various numerical experiments are illustrated to show the performance and advantages of the proposed method.*

## 1. Introduction

Image segmentation is important in image processing and computer vision. It has been an active research area and numerous methods have been proposed, see [2, 3, 4, 16] and the references therein. However, it is a challenging task to segment the object of interest precisely and accurately for poor quality images, such as occlusion and low contrast

images. Image segmentation with shape priors, such as convexity [8], star shape [26], geodesic star [9], hedgehog [11], can effectively improve the segmentation accuracy and precision. Convexity is one of the widely used shape priors [7, 8, 19]. In this paper, we propose a continuous model for multiple disjoint convex objects segmentation. Our method is based on convexity shape representation by level set function. One important advantage of the proposed model is that its computational cost is independent of the number of objects. We only need one level set function to represent the convexity all the considered convex objects. The convexity of the represented objects is equivalent to a simple constraint on the signed distance function. Labels on foreground and background can be incorporated in the model easily to improve the segmentation accuracy. Some special techniques are used to combine ADMM and proper boundary conditions to get very efficient algorithm. Experiments on various images show the effectiveness of the model and the efficiency of the algorithms.

**Related works:** Image segmentation with convex shape prior has attracted much attention. It is well-known that convexity is an important cue for human vision [12, 15]. Many objects in optical images and images created from some inverse problems (such as CT, ultrasound, MRI, sonic) are convex. However, the object integrity is often broken due to occlusions, illumination bias and artifacts caused by inverse crimes. In order to tackle the problem, convexity prior has been investigated for image segmentation.

Several methods have been proposed in the literature. According to the definition of convex region, the authors of

[8] propose a discrete method for binary segmentation by penalizing 1-0-1 configurations on all the intervals of any straight line passing through any pixel in certain directions. Such penalization terms are non-submodular and they make the related optimization problem difficult to solve. Trust region (TR) method is used to solve the model after linear or quadratic approximation. Similarly, 0-1-0 configurations on straight lines are used to compute the integral of squared curvature along object boundary [17].

In [22], a method for  $n$ -sided convex object modelling is proposed. This method needs one foreground and  $n$  background labels. Therefore, the labeling number is very large, and the computation cost is very expensive for complex objects, e.g. a circle.

It is a natural way to represent shape priors by level set function [5, 18]. For convex shape segmentation, one only needs to keep the curvature nonnegativity of the boundary curve. The curvature of the boundary curve can be computed easily using level set representation. This idea is adopted for convex segmentation in the literature [2, 25, 28]. The method is further developed in [13, 27], where the convexity of the level set function (signed distance function) is guaranteed by imposing proper constraints, and efficient algorithms are developed.

As for the multiple convex objects segmentation problem, it is more challenging than single convex object segmentation. In [7], the method for single convex object segmentation in [9] is extended for multiple convex objects segmentation. Graph-cut algorithm is developed to solve the TR sub-problem, which can maintain the convexity of all foreground subregions simultaneously. In [19], the min-cost multi-cut method is extended for multiple convex objects segmentation. The objects convexity is obtained by imposing constraint on the number of intersections of any line with the object boundary. Branch-cut of ILP solver is used to solve it.

Recently,  $k$ -part shape priors for image segmentation drew a lot of attentions [10, 14, 29]. The aim of these methods is to divide the object into several parts with given shape priors. The notions of  $k$ -convexity [1] and  $k$ -star shape [23] are introduced. This concept is extended in [10] for any shape priors, such as geodesic-star and hedgehog.

**Our contributions:** The segmentation problem for multiple convex objects is a challenging task. There are not so many methods that are easy to use, efficient and robust for real applications. For the methods in [7, 19], plenty of labels on the objects and backgrounds are usually needed to get accurate segmentation results, and the computational cost is high, especially for large number of objects. In this paper, we propose a level set representation method to segment multiple convex objects. The proposed method has three advantages as follows.

1) The convexity of the segmented objects is guaranteed by

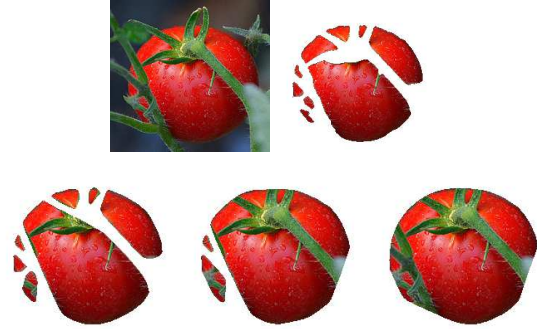


Figure 1. Results by the proposed method with different values of  $c$  (second row,  $c = 2, 2.3, 2.5$  from left to right) and the method without (top right) convexity prior for the tomato image (top left).

a linear constraint on the signed distance function associated to the union of all the objects. Thus, only one level set function is needed for our method regardless of the number of objects. The computational cost does not increase with the increasing of the number of objects.

2) The proposed method is based on the property of  $c$ -sublevel set (see Section 2) corresponding to the union of convex objects. The parameter can be easily tuned to merge and separate objects based on the shortest distance between them (see Figure 1).

3) We develop special techniques to solve the minimization problem with the signed distance function under the convexity constraint. This has led to an efficient algorithm by dividing the problem into easily solved sub-problems.

We explain in more details about the proposed method as follows. Usually, we need  $k$  convex level set functions to represent  $k$  convex objects. In this work, we prove that the convexity of  $k$  objects can be characterized by the property of the  $c$ -sublevel set of the SDF equivalently, i.e. the  $c$ -sublevel set consists of  $k$  convex subregions if  $c$  is less than half of the smallest distance,  $\tilde{c}$ , between any two objects. Such characterization provides a description of the convexity of the  $k$  convex objects, i.e. the SDF corresponding to their union should be convex on each subregion of its  $c$ -sublevel set. On the other hand, the SDF is convex on each subregion if and only if the curvature (Laplacian of SDF) of the SDF's  $c$  level set curve is nonnegative for  $c < \tilde{c}$ .

The result on the level set representation for multiple convex objects is incorporated with probability based method for multiple convex objects segmentation, i.e. a nonnegative constraint of Laplacian SDF is imposed on the  $c$ -sublevel set instead of the whole image domain [13, 27]. For simplicity, Gaussian mixture method (GMM) is adopted to compute the probabilities belonging to the background and foreground for each point. We adopt the method in [7] to compute the probability for foreground containing all the convex objects, i.e. we don't distinguish the distributions for different objects. This method can reduce the model

complexity and computational cost. For poor quality images, labels on the foreground and background can be added to improve the segmentation accuracy. Even more, we can choose different values of the parameter  $c$  to merge or separate adjacent objects (see Figure 1). This will be discussed in Section 2.

Traditionally solving minimization problems with signed distance functions is time-consuming. Recent work [6] reveals that one can use ADMM type of methods to obtain very fast algorithms for such problems. In this paper, we develop an efficient algorithm for our proposed model. Proper boundary conditions and suitable splitting of the variables are essential to reduce the complicated optimization problem into simpler sub-problems. Our experiments not only verify the effectiveness of the proposed method in segmentation while keeping the convexity of the object regions, but also demonstrate its robustness against noise and parameter imprecision.

The rest of this paper is organized as follows. In Section 2 we provide our method in details, from the setup to the mathematical framework, and present the ADMM algorithm for our model in Section 3. In Section 4 we show some numerical examples, which demonstrate the effectiveness of the proposed method. Finally, conclusions and future work are discussed in Section 5.

## 2. Method description

In this section we present the method for multiple objects segmentation using a single level set function under the convexity prior. First we shall discuss the representation method of multiple convex objects by a single level set function. Later we shall incorporate such representation with the GMM-based segmentation model.

### 2.1. Convex shape representation

Assume  $D \subset \mathbb{R}^2$  (possibly consisting of several disjoint connected subregions). The signed distance function (SDF) of  $D$  is defined as follows:

$$\phi(x) = \begin{cases} -\text{dist}(x, \partial D) & x \in D \\ \text{dist}(x, \partial D) & x \notin D, \end{cases} \quad (1)$$

where  $\partial D$  denotes the boundary of  $D$  and  $\text{dist}(x, \partial D) = \min_{y \in \partial D} \|x - y\|_2$ . It is well known that  $|\nabla \phi| = 1$  holds almost everywhere for the SDF of any region. For a given function  $\psi$ , the level set and sublevel set are defined as

$$\begin{aligned} \text{lev}_\psi^c &= \{x | \psi(x) = c\}, \\ \text{slev}_\psi^c &= \{x | \psi(x) \leq c\}. \end{aligned}$$

It is obvious that  $\partial D = \text{lev}_\phi^0$  and  $D = \text{slev}_\phi^0$ .

In the following, we assume  $D = \bigcup_{k \in \mathbb{K}} \Omega_k$ , where  $\Omega_k$  for  $k \in \mathbb{K} = \{1, 2, \dots, K\}$  are disjoint simple regions. In

addition, we define the distance between any two convex regions  $\Omega_i, \Omega_j$  ( $i \neq j$ ) as

$$\text{dist}(\Omega_i, \Omega_j) = \min\{\|x - y\|_2, x \in \Omega_i, y \in \Omega_j\}. \quad (2)$$

Then we have the following result about the relation between the convexity of  $\Omega_k, k \in \mathbb{K}$ , and the level set function  $\phi$  corresponding to  $D$ .

**Lemma 1** *Assume  $\Omega_k \subset \mathbb{R}^2, k \in \mathbb{K}$  are disjoint simply connected regions, and  $\phi$  is the SDF of  $D = \bigcup_{k=1}^K \Omega_k$ . Let  $\tilde{c} = \frac{1}{2} \min\{\text{dist}(\Omega_i, \Omega_j), i \neq j, i, j \in \mathbb{K}\}$ . Then all  $\Omega_k, k \in \mathbb{K}$ , are convex if and only if  $\text{slev}_\phi^c$  consists of  $K$  convex subregions  $\Omega_k^c = \bar{\Omega}_k \cap \text{slev}_\phi^c, k \in \mathbb{K}$ , for all  $c < \tilde{c}$ , where  $\bar{\Omega}_k = \{x | \text{dist}(x, \Omega_k) < \tilde{c}\}$ .*

The proof of Lemma 1 is given in Appendix. According to Lemma 1, level set  $\text{lev}_\phi^c = \partial \text{slev}_\phi^c$  for all  $c < \tilde{c}$  consists of  $K$  convex curves  $\partial \Omega_k^c$  (some may be empty sets). It is well known that the curve convexity is equivalent to the nonnegativity of its curvature. Due to  $|\nabla \phi(x)| = 1$  almost everywhere, the curvature for the  $c$  level set of SDF  $\phi$  is

$$\kappa(c) = \nabla \cdot \left( \frac{\nabla \phi}{|\nabla \phi|} \right) = \Delta \phi. \quad (3)$$

Therefore, we have  $\Delta \phi(x) \geq 0$  if  $\phi(x) < \tilde{c}$ . This yields the following key theorem.

**Theorem 1** *Assume  $\Omega_k \subset \mathbb{R}^2, k \in \mathbb{K}$  are disjoint simply connected regions, and  $\phi$  is the SDF corresponding to  $D = \bigcup_{k=1}^K \Omega_k$ . Let  $\tilde{c} = \frac{1}{2} \min\{\text{dist}(\Omega_i, \Omega_j), i \neq j, i, j \in \mathbb{K}\}$ . Then all  $\Omega_k, k \in \mathbb{K}$ , are convex if and only if  $\Delta \phi \geq 0$  almost everywhere on  $\text{slev}_\phi^c$  for  $c < \tilde{c}$ .*

For an optimization problem with SDF (e.g. level set based image segmentation model), if we require  $\Delta \phi \geq 0$  on  $\text{slev}_\phi^c$  for  $c \geq 0$ , we will get a SDF  $\phi$  such that  $\text{slev}_\phi^0$  consists of several convex subregions by Theorem 1, and the distance between any two subregions will be larger than  $2c$ . In other words, if there are two regions, the distance between which is smaller than  $2c$ , they must be contained in one of the subregions of  $\text{slev}_\phi^0$ .

### 2.2. Image segmentation model with convexity shape constraint

In this subsection, we describe the Gaussian mixture method (GMM) for multiple disjoint objects segmentation with convex shape prior using a single level set function. The proposed method differs slightly from the traditional GMM-based model. Although we estimate the Gaussian distributions on different objects, we don't distinguish them in the model but view their mixture as the distribution of foreground.

Assume an image  $I : x \in \Omega \subset \mathbb{R}^2 \mapsto [0, 1]^d$  with  $d = 1$  for gray image and  $d = 3$  for color image. Suppose that the object regions  $\Omega_k \subset \Omega, k \in \mathbb{K}$ , that we would like to segment are convex. Let  $\Omega_0 = \Omega \setminus (\bigcup_{k=1}^K \Omega_k)$  be the background region. Suppose the values  $I(x)$  on  $\Omega_k, k \in \mathcal{K} = \{0, 1, \dots, K\}$ , obey the Gaussian distribution  $G(\mu_k, \Sigma_k)$ , and denote the probability density function by

$$p(I(x), \mu_k, \Sigma_k) = \frac{1}{A} \exp\left(-\frac{\|I(x) - \mu_k\|_{\Sigma_k^{-1}}^2}{2}\right), \quad (4)$$

where  $A = (2\pi)^{\frac{d}{2}} \det(\Sigma_k)^{1/2}$ . Then the proportion of the  $k$ -th distribution is  $r_k = \frac{|\Omega_k|}{|\Omega|}, k \in \mathcal{K}$ . In this work, the probabilities of point  $x$  belonging to the background  $\Omega_0$  and foreground  $\bigcup_{k=1}^K \Omega_k$  are

$$p_0(x) = \frac{r_0 p(I(x), \mu_0, \Sigma_0)}{\sum_{k=1}^K r_k p(I(x), \mu_k, \Sigma_k)}, \quad (5)$$

and  $p_1(x) = 1 - p_0(x)$ , respectively. Assume  $\phi$  is the SDF corresponding to  $\bigcup_{k=1}^K \Omega_k$ , and  $H$  is the Heaviside function, i.e.  $H(t) = 0$  for  $t \leq 0$  and 1 otherwise. We have

$$p(\phi) = \prod_{x \in \Omega} [p_0(x)]^{H(\phi(x))} [1 - p_0(x)]^{1 - H(\phi(x))}. \quad (6)$$

Discarding the constant term, we can get the log-likelihood functional

$$- \int_{\Omega} [\ln(1 - p_0(x)) - \ln p_0(x)] H(\phi(x)) dx. \quad (7)$$

The nonnegative weighted likelihood functional is used as the region force term of the following image segmentation model

$$\arg \min_{\phi} \int_{\Omega} [-w_0 \ln p_0(x) + w_1 \ln(1 - p_0(x))] H(\phi) dx + \int_{\Omega} g(x) \delta(\phi) |\nabla \phi| dx, |\nabla \phi(x)| = 1, x \in \Omega, \quad (8)$$

where  $g = \frac{\alpha}{1 + \beta |\nabla \hat{I}(x)|}$  is an edge detector function with  $\hat{I}$  being the smoothing image of  $I$  and  $\alpha, \beta > 0$ ,  $\delta$  is the distribution derivative of  $H$ , and  $w_0, w_1 > 0$  are balance parameters. The constraint  $|\nabla \phi(x)| = 1$  is required for SDF. In the following, we denote

$$F(\phi) = [-w_0 \ln p_0(x) + w_1 \ln(1 - p_0(x))] H(\phi) + g(x) \delta(\phi).$$

Based on Theorem 1, we can obtain the following model for multiple objects segmentation with convexity prior by imposing constraint  $\Delta \phi \geq 0$  on  $\text{slev}_{\phi}^c$

$$\arg \min_{\phi} \int_{\Omega} F(\phi) dx, \Delta \phi(x) \geq 0, x \in \text{slev}_{\phi}^c, |\nabla \phi(x)| = 1, x \in \Omega, \quad (9)$$

where  $c \geq 0$  is a small user-specified parameter, which may vary for different images and desired segmentation results.

As for the choice of  $c$ , we can use  $c = 0$  for simplicity in practice. However, we can choose large value for  $c$  if there is only one object to segment. In addition, we can select  $c$  deliberately to get desired result.

We can see the role of  $c$  clearly by comparing the segmentation results in Figure 1. As we see that the red tomato is completely separated into several (approximate) convex regions by green branches. Therefore, the result by convex shape prior model (9) with  $c = 0$ , which is not illustrated here, is very similar with the one by the model (8) without convex shape prior. However, these disjoint convex regions will be gradually merged with the increasing of parameter  $c$ , which is just the thing that Theorem 1 tells us.

Labeling information is widely used for convex object segmentation [7, 8, 14]. Our method also can incorporate labeling information. Assume  $L_{bg}$  and  $L_{ob}$  are the labeled regions on the background and foreground. Then the solution of SDF should satisfy  $\phi(x) \geq 0$  for  $x \in L_{bg}$  and  $\phi(x) \leq 0$  for  $x \in L_{ob}$ . We only need to add an additional constraint on the optimization problem (9), and get the following minimization problem with labeling prior.

$$\arg \min_{\phi} \int_{\Omega} F(\phi) dx, \Delta \phi(x) \geq 0, x \in \text{slev}_{\phi}^c, |\nabla \phi(x)| = 1, x \in \Omega, \phi \in \mathbb{L}, \quad (10)$$

where  $\mathbb{L} = \{\psi | \psi(x) \geq 0, x \in L_{bg}, \text{ and } \psi(x) \leq 0, x \in L_{ob}\}$ .

### 3. Algorithm for the proposed models

In this section the ADMM algorithm for the constrained optimization problem (10) is presented in details, and the algorithms for (8) and (9) can be obtained similarly. For implementation simplicity, we assume the boundary of the image domain  $\Omega$  belongs to the background, all the object regions of interest are in the interior of the image domain. Otherwise we can always pad extra pixels just outside the boundary of the image domain. Thus we only require  $\phi$  to be a signed distance function inside the interior set  $\Omega^o$  of  $\Omega$ , and  $\Delta \phi \geq 0$  on  $\text{slev}_{\phi}^c$ , i.e.

$$|\nabla \phi(x)| = 1, x \in \Omega^o \text{ and } \Delta \phi(x) \geq 0, x \in \text{slev}_{\phi}^c. \quad (11)$$

In order to obtain the efficient algorithm, we impose the following conditions of  $\phi$  on the boundary of  $\Omega$

$$\frac{\partial \phi}{\partial \vec{n}} = \frac{\partial \Delta \phi}{\partial \vec{n}} = 0, \text{ on } \partial \Omega. \quad (12)$$

Here and after, we denote by  $\vec{n}$  the unit outer normal vector of  $\partial\Omega$ , and define the following function spaces and sets

$$\begin{aligned} V &= \{\phi \in H^2(\Omega) \mid \frac{\partial\phi}{\partial\vec{n}} = \frac{\partial\Delta\phi}{\partial\vec{n}} = 0 \text{ on } \partial\Omega\}, \\ V_1 &= \{\zeta \in H^1(\Omega) \mid \frac{\partial\zeta}{\partial\vec{n}} = 0 \text{ on } \partial\Omega\}, \\ V_2 &= \{\xi \in H^1(\Omega) \times H^1(\Omega) \mid \xi \cdot \vec{n} = 0 \text{ on } \partial\Omega\}, \\ S_0 &= \{\psi \mid \psi \in V, \psi \in \mathbb{L}\}, \\ S_1 &= \{\zeta \in V_1 \mid \zeta(x) \geq 0, x \in \text{slev}_\phi^c\}, \\ S_2 &= \{\xi \in V_2 \mid |\xi(x)| = 1, x \in \Omega^o\}. \end{aligned}$$

By introducing three auxiliary variables  $\psi = \phi, \zeta = \Delta\phi$  and  $\xi = \nabla\phi$ , the constrained minimization problem (10) under (11) and (12) is equivalent to:

$$\begin{cases} \arg \min_{\phi, \zeta, \xi} \int_{\Omega} F(\phi) dx, \frac{\partial\phi}{\partial\vec{n}} = \frac{\partial\Delta\phi}{\partial\vec{n}} = 0, \text{ on } \partial\Omega \\ \psi = \phi, \zeta = \Delta\phi, \xi = \nabla\phi, \psi \in S_0, \zeta \in S_1, \xi \in S_2. \end{cases} \quad (13)$$

The augmented Lagrangian functional for problem (13) is then given as

$$\begin{aligned} L(\phi, \psi, \xi, \zeta, \lambda_0, \lambda_1, \lambda_2) &= \int_{\Omega} F(\phi) dx \\ &+ \langle \lambda_0, \phi - \psi \rangle + \langle \lambda_1, \Delta\phi - \zeta \rangle + \langle \lambda_2, \nabla\phi - \xi \rangle \\ &+ \frac{\rho_0}{2} \|\phi - \psi\|_2^2 + \frac{\rho_1}{2} \|\Delta\phi - \zeta\|_2^2 + \frac{\rho_2}{2} \|\nabla\phi - \xi\|_2^2, \end{aligned} \quad (14)$$

where  $\phi, \lambda_0 \in V, \lambda_1, \zeta \in V_1, \lambda_2, \xi \in V_2, \psi \in S_0, \zeta \in S_1, \xi \in S_2$ , and  $\rho_0, \rho_1, \rho_2 > 0$  are augmented parameters. We use  $\langle \cdot, \cdot \rangle$  to denote the inner product of two functions in  $L^2(\Omega)$ . The ADMM algorithm for (13) is now given in Algorithm 1. If there is no labeling information, we view

---

**Algorithm 1** Alternating direction algorithm for (14)

---

1. Initialization:  $\lambda_i = 0, \rho_i > 0, i = 0, 1, 2$ , and  $\phi^0$ ;
  3. For  $t = 0, 1, 2, \dots, \text{Num}$
  4.  $\psi^{t+1} = \arg \min_{\psi \in S_0} L(\phi^t, \psi, \xi^t, \zeta^t, \lambda_0^t, \lambda_1^t, \lambda_2^t)$ ,
  5.  $\zeta^{t+1} = \arg \min_{\zeta \in S_1} L(\phi^t, \psi^{t+1}, \xi^t, \zeta, \lambda_0^t, \lambda_1^t, \lambda_2^t)$ ,
  6.  $\xi^{t+1} = \arg \min_{\xi \in S_2} L(\phi^t, \psi^{t+1}, \xi, \zeta^{t+1}, \lambda_0^t, \lambda_1^t, \lambda_2^t)$ ,
  7.  $\phi^{t+1} = \arg \min_{\phi \in V} L(\phi, \psi^{t+1}, \xi^{t+1}, \zeta^{t+1}, \lambda_0^t, \lambda_1^t, \lambda_2^t)$ ,
  8.  $\lambda_0^{t+1} = \lambda_0^t + \rho_0(\phi^{t+1} - \psi^{t+1})$ ,
  9.  $\lambda_1^{t+1} = \lambda_1^t + \rho_1(\Delta\phi^{t+1} - \zeta^{t+1})$ ,
  10.  $\lambda_2^{t+1} = \lambda_2^t + \rho_2(\nabla\phi^{t+1} - \xi^{t+1})$ ,
  11. end(for)
- 

$L_{bg}$  and  $L_{ob}$  as empty sets. For this case, the terms with respect to  $\psi$  is maintained as well and understood as a proximal term about  $\phi$  to stabilize the iteration procedure. The role of it will be clear for the update of  $\phi$  in (19).

Steps 4, 5 and 6 have closed form solutions, and the minimizer of Step 7 is the solution of a fourth order partial differential equation (PDE), which can be converted to

two 2nd order PDEs and they can be solved efficiently using the discrete cosine transform (DCT) [21].

♠  $\psi, \zeta, \xi$  updates in Steps 4, 5 and 6: For the solution  $\psi^{t+1}$ , after simply calculating and discarding the terms not related to  $\psi$ , we can get

$$\psi^{t+1} = \arg \min_{\psi \in S_0} \frac{\rho_0}{2} \|\psi - \tilde{\psi}^t\|_2^2, \quad (15)$$

where  $\tilde{\psi}^t = \phi^t(x) + \lambda_0^t(x)/\rho_0$ . According to the constraint of  $\mathbb{L}$ , we can obtain the solution  $\psi^{t+1}$  as follows:

$$\psi^{t+1}(x) = \begin{cases} \max\{0, \tilde{\psi}^t(x)\} & x \in L_{bg} \\ \min\{0, \tilde{\psi}^t(x)\} & x \in L_{ob} \\ \tilde{\psi}^t(x) & \text{otherwise.} \end{cases} \quad (16)$$

Similarly, we can get the solution to Step 5,

$$\zeta^{t+1}(x) = \begin{cases} \max\{0, \tilde{\zeta}^t(x)\} & x \in \text{slev}_{\phi^t}^c \\ \tilde{\zeta}^t & x \notin \text{slev}_{\phi^t}^c, \end{cases} \quad (17)$$

where  $\tilde{\zeta}^t(x) = \Delta\phi^t(x) + \lambda_1^t(x)/\rho_1$ . Using the constraint  $|\xi^{t+1}(x)| = 1$ , we can obtain the solution of  $\xi^{t+1}$  as follows:

$$\xi^{t+1}(x) = \begin{cases} \tilde{\xi}^t(x)/|\tilde{\xi}^t(x)| & x \in \Omega^o \\ \tilde{\xi}^t(x) & x \in \Omega \setminus \Omega^o, \end{cases} \quad (18)$$

where  $\tilde{\xi}^t(x) = \nabla\phi^t(x) + \lambda_2^t(x)/\rho_2$ .

♠  $\phi$  update in Step 7: Based on the assumptions  $\lambda_1^t, \zeta^{t+1} \in V_1, \lambda_2^t, \xi^{t+1} \in V_2$  and  $\phi^{t+1}, \psi^{t+1}, \lambda_0^t \in V$ , we have

$$\begin{aligned} \frac{\partial\gamma}{\partial\vec{n}} = \frac{\partial\Delta\gamma}{\partial\vec{n}} = 0, \gamma &= \phi^{t+1}, \psi^{t+1}, \lambda_0^t \\ \frac{\partial\zeta^{t+1}}{\partial\vec{n}} = \frac{\partial\lambda_1^t}{\partial\vec{n}} = 0, \xi^{t+1} \cdot \vec{n} &= \lambda_2^t \cdot \vec{n} = 0 \end{aligned}$$

hold on  $\partial\Omega$ . We can obtain the Euler Lagrange equation of the objective functional in Step 7

$$\begin{cases} \rho_1\Delta^2\phi^{t+1} - \rho_2\Delta\phi^{t+1} + F'(\phi^{t+1}) + \rho_0\phi^{t+1} = \text{rhd}^t \text{ in } \Omega \\ \frac{\partial\phi^{t+1}}{\partial\vec{n}} = 0, \frac{\partial\Delta\phi^{t+1}}{\partial\vec{n}} = 0, \text{ on } \partial\Omega, \end{cases}$$

where  $\text{rhd}^t = \rho_0\psi^{t+1} - \lambda_0^t - \Delta(\lambda_1^t - \rho_1\zeta^{t+1}) - \nabla^T(\lambda_2^t - \rho_2\xi^{t+1})$ , and  $\nabla^T$  denotes the conjugate operator of  $\nabla$ . Approximating the nonlinear term  $F(\phi^{t+1})$  by  $F(\phi^t)$ , we can get an approximation solution by solving

$$\begin{cases} \rho_1\Delta^2\phi^{t+1} - \rho_2\Delta\phi^{t+1} + \rho_0\phi^{t+1} = \text{RHD}^t \\ \frac{\partial\phi^{t+1}}{\partial\vec{n}} = 0, \frac{\partial\Delta\phi^{t+1}}{\partial\vec{n}} = 0, \text{ on } \partial\Omega, \end{cases} \quad (19)$$

where  $\text{RHD}^t = \text{rhd}^t - F'(\phi^t)$ . Selecting  $\rho_i$  ( $i = 0, 1, 2$ ) satisfying  $\rho_2 = 2\sqrt{\rho_0\rho_1}$ , we can rewrite (19) as

$$\begin{cases} (\sqrt{\rho_1}\Delta - \sqrt{\rho_0}I)^2\phi^{t+1} = \text{RHD}^t \\ \frac{\partial\phi^{t+1}}{\partial\vec{n}} = 0, \frac{\partial\Delta\phi^{t+1}}{\partial\vec{n}} = 0, \text{ on } \partial\Omega, \end{cases} \quad (20)$$

which can be converted to two Laplacian equations

$$\begin{cases} (\sqrt{\rho_1}\Delta - \sqrt{\rho_0}I)\varphi^{t+1} = \text{RHD}^t \\ \frac{\partial\varphi^{t+1}}{\partial\bar{n}} = 0, \end{cases} \quad (21)$$

$$\begin{cases} (\sqrt{\rho_1}\Delta - \sqrt{\rho_0}I)\phi^{t+1} = \varphi^{t+1} \\ \frac{\partial\phi^{t+1}}{\partial\bar{n}} = 0. \end{cases} \quad (22)$$

We can solve equations (21) and (22) by DCT efficiently (details can be found in [13]).

The numerical implementations for (16)-(18) can be got easily after discretizing the image domain. For the numerical solution to (22), we use  $H_\epsilon(\phi) = \frac{1}{2} + \frac{1}{\pi} \arctan(\phi/\epsilon)$  and  $\delta_\epsilon(\phi) = H'_\epsilon(\phi) = \frac{\epsilon}{\epsilon^2 + \phi^2}$  to approximate  $H(\phi)$  and  $\delta(\phi)$  for the computation of  $F'$ , where  $\epsilon > 0$  is a small number.

In addition, we need to update the region force term by estimating the means and variances of Gaussian distributions. Let  $\phi^t$  be the level set function at present. The background domain is  $\Omega_0 = \{x | \phi(x) > 0\}$ . For the object domains,  $\text{slev}_\phi^0$  is separated into several disconnected subregions  $\Omega_k, k \in \mathbb{K}$ , and the parameters are estimated on the subregions.

## 4. Experiments

A lot of experiments on various images are conducted to verify the effectiveness of the proposed methods with and without convexity prior. These experiments show that the proposed convexity model can yield convex results. Some of the experiments are demonstrated as follows.

Some parameters in the models and algorithms are the same for all examples below. We choose  $\alpha = 0.1, \beta = 1$  for the edge detection function  $g, \rho_0 = 1, \rho_1 = 0.5, \epsilon = 0.5$  for the numerical implementation. For the convexity models (9) and (10),  $c = 0$  is used for all the examples below if it is not specified. In addition, the parameters  $w_0, w_1$  in the proposed models (9) and (8) with and without convexity prior are chosen to be same for the same image. For all examples, the number of objects,  $K$ , is user-specified.

We use two methods to initialize  $\phi$ . The initial object regions is estimated by  $k$ -means clustering method (Figures 2, 4, 6 and 7), or initial object boundaries (circles for example) are given on the objects manually (Figures 3 and 5). Then the SDF corresponding to the region estimate or initial boundaries is computed by the fast marching method [20] or the fast sweeping method [24, 30]. The experiments show that our method is robust to the initialization of  $\phi$ .

### 4.1. Single object

Figure 2 illustrates the segmentation results for three real images, ultrasound image of embryo (top), sonar image of shipwreck (middle) and image of fossil leaf (bottom). They represent three kinds of challenging images for the exiting segmentation methods because the object regions are

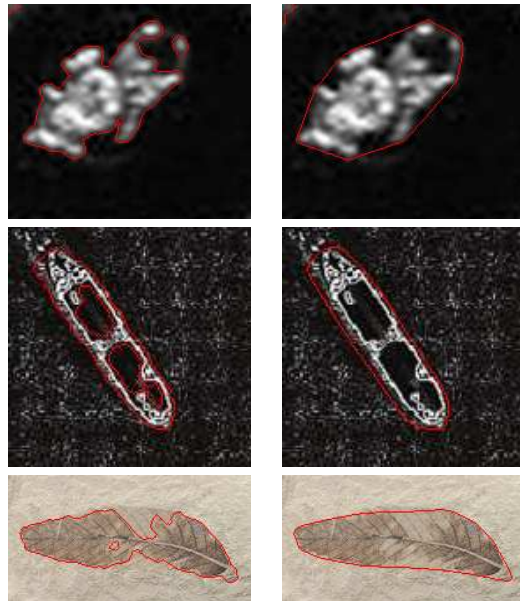


Figure 2. Results for one object. The results by (8) and (9) are in the first and second columns, respectively.

incomplete due to poor imaging qualities: The embryo is broken into several parts because of low quality, the shipwreck is shown with black holes because of no sound reflection signal, and the values of fossil leaf on some regions are faded and similar to these on the background rather than the leaf region. Therefore, it is very difficult for the image segmentation model without shape prior to get correct results. The parameters  $[w_0, w_1]$  for the three examples from top to bottom are  $[0.2, 0.1], [0.2, 0.1]$  and  $[0.1, 0.1]$ . The results show that the proposed convexity method (9) can yield the segmentation results correctly, while the method (8) without convexity prior fails to get the whole object regions.

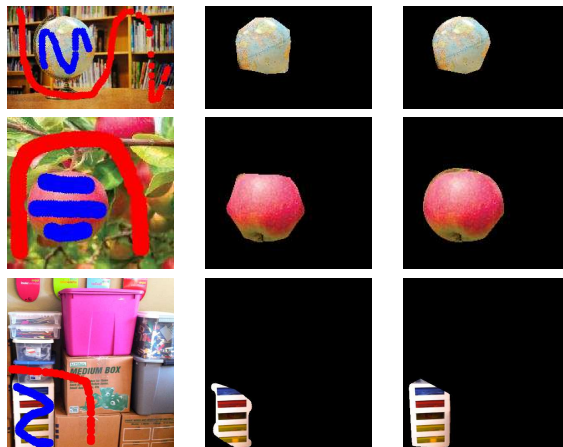


Figure 3. Comparison with the method in [8].

Figure 3 shows three examples to compare our method (10) with the one in [8]. The labeled images (left) and

the results by [8] (center) are downloaded from website <http://vision.csd.uwo.ca/code/>. The results by the proposed method using the same labels are presented on the right. We can see that the results by our method are better than these by the method in [8] visually. For example, the result of bottom image by the method [8] is nonconvex obviously, while the result by our method is convex. For these images in Figure 3, the nonnegativity constraint on Laplacian  $\phi$  is imposed on the whole image except the image domain boundary because there is only one object to segmentation.

#### 4.2. Multiple objects

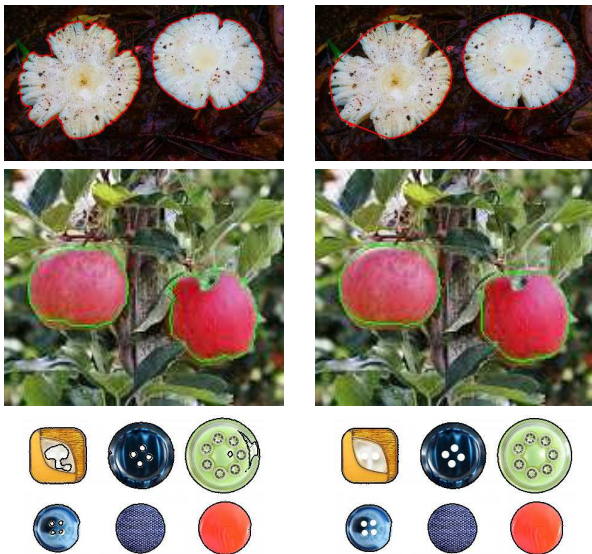


Figure 4. Results for multiple objects segmentation. Left column: results by the method (8). Right column: results by the method (9). The parameters  $[w_0, w_1]$  for the three images from top to bottom are  $[0.2, 0.1]$ ,  $[0.1, 0.08]$ ,  $[0.2, 0.1]$ , respectively.

The segmentation results of three images containing more than one objects are illustrated in Figure 4. The results in Figure 4 show that the proposed method can be used for multiple objects segmentation using a single SDF as long as they are disjunct. The integrity of the objects, mushrooms, apples and clothe buttons, are broken due to physical factors, such as occlusion and illumination bias. Therefore, the method (8) without shape prior fails to get the original objects' boundaries, and it is difficult to identify them from the segmentation results by (8) automatically. On the other hand, the results by the proposed convex segmentation method (9) can catch the ideal boundaries of the objects.

Figure 5 displays an example to compare the proposed method (10) with the method in [7]. The labeled image (left) and the segmentation result by [7] (middle) are cropped from [7]. The result by our method is presented on right. We can see that the result by our method is better than



Figure 5. Comparison with the method in [7].

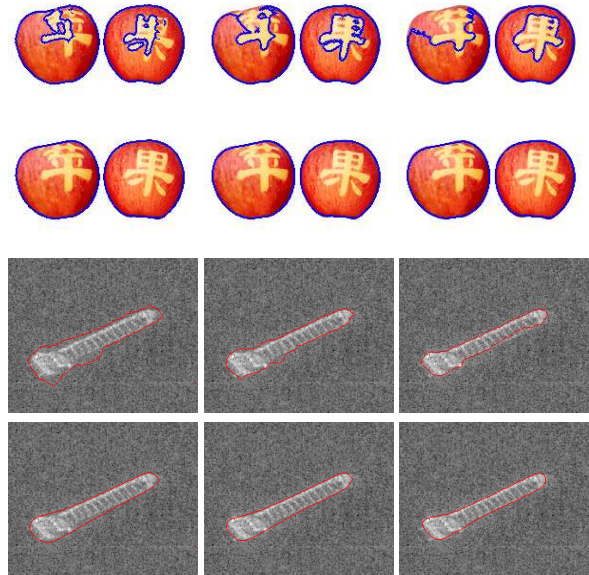


Figure 6. First and third rows: Results by the model (8) without convexity prior. Second and fourth rows: Results by the convexity model (9).

the one in [7] (see the region in the ellipse).

#### 4.3. Sensitivity to parameters $w_0, w_1$ and noise

In this subsection, we will investigate the sensitivity of the proposed models with and without convex shape prior to noise and values of  $w_0$  and  $w_1$ . Figure 6 illustrates the segmentation results of two real images with different parameter pairs  $w_0, w_1$ . The parameters  $[w_0, w_1]$  are  $[0.1, 0.4]$ ,  $[0.1, 0.5]$  and  $[0.1, 0.6]$  for apple image and  $[0.1, 0.1]$ ,  $[0.1, 0.2]$  and  $[0.1, 0.4]$  for the remote image of a ship from left to right. These results show that the convexity model (9) is more stable to the parameter imprecision than the one (8) without convexity prior.

Segmentation results of noisy images, which are heavily polluted by Gaussian noises, are shown in Figure 7. The noise levels are about 30, 50%, respectively, and the parameters  $w_0 = 0.2, w_1 = 0.15$  are kept the same for both. We can see that the boundaries of the segmented objects by the convexity model (9) are convex and smooth, while the boundaries of the result by the model (8) without convex shape prior are rough due to noise effect. Such experiment shows that the convexity model (9) is more stable to noise pollution than the model (8) without convexity prior. Although the Chinese old coins are not convex, we can ob-

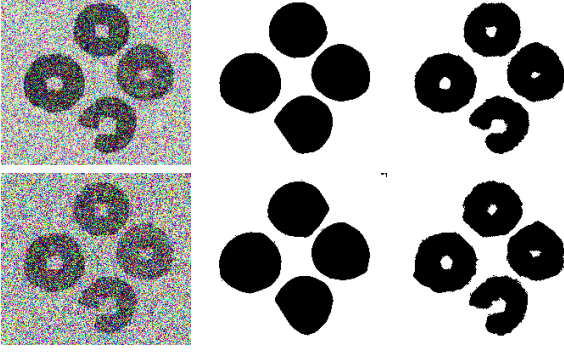


Figure 7. Original image, results by convexity model (9) and model (8) without convex shape prior are shown from left to right, respectively.

tain convex results due to the convex constraints, which also shows the effectiveness of the proposed method.

## 5. Conclusion

In this work, we propose a method to represent multiple convex objects by single level set function, and show its application in multi-object segmentation with convexity shape prior. Various experiments not only verify the effectiveness of the proposed method, but also show the stability of the method to noise and parameter choices. In the future, we will develop more efficient algorithm to implement the proposed model and investigate other methods for image segmentation with convexity prior.

## Appendix: Proof to Lemma 1

The sufficiency is very easy to obtain by letting  $c = 0$ . We prove the necessity only. Let  $\bar{D} := \bigcup_{k=1}^K \bar{\Omega}_k$ . Due to  $\text{slev}_\phi^c \subset \text{slev}_\phi^{\tilde{c}}$  for  $c \leq \tilde{c}$  and  $\text{slev}_\phi^{\tilde{c}} = \bar{D}$ , we have

$$\text{slev}_\phi^c = \text{slev}_\phi^c \cap \bar{D} = \text{slev}_\phi^c \cap \left( \bigcup_{k=1}^K \bar{\Omega}_k \right) = \bigcup_{k=1}^K (\text{slev}_\phi^c \cap \bar{\Omega}_k).$$

It is obvious that  $\Omega_k^c = \text{slev}_\phi^c \cap \bar{\Omega}_k$ ,  $k \in \mathbb{K}$ , are disjoint because  $\bar{\Omega}_k$ ,  $k \in \mathbb{K}$ , are disjoint according to the assumption. Therefore, it is sufficient to prove that  $\Omega_k^c$  for each  $k \in \mathbb{K}$  is convex. Because  $\Omega_k^c \subset \text{slev}_\phi^c$  ( $k \in \mathbb{K}$ ) are disjoint, we can prove them one by one. Without loss of generality, we prove that  $\Omega_1^c$  is convex.

For any  $x_1, x_2 \in \Omega_1^c \subset \bar{\Omega}_1$ , we should prove that  $[\lambda, x_1, x_2] := \lambda x_1 + (1 - \lambda)x_2 \in \Omega_1^c = \text{slev}_\phi^c \cap \bar{\Omega}_1$  for all  $\lambda \in [0, 1]$ . We need to prove two arguments (I)  $[\lambda, x_1, x_2] \in \bar{\Omega}_1$  and (II)  $[\lambda, x_1, x_2] \in \text{slev}_\phi^c$ , respectively.

(I) In fact, assume  $y_1, y_2 \in \Omega_1$  such that

$$\text{dist}(x_i, y_i) = \text{dist}(x_i, \Omega_1) = \min_{y \in \Omega_1} \|x_i - y\|_2 < \tilde{c}, i = 1, 2.$$

According to the convexity assumption of  $\Omega_1$  and triangle inequality, we have  $[\lambda, y_1, y_2] \in \Omega_1$  and

$$\begin{aligned} \text{dist}([\lambda, x_1, x_2], \Omega_k) &\leq \|[\lambda, x_1, x_2] - [\lambda, y_1, y_2]\|_2 \\ &\leq [\lambda, \|x_1 - y_1\|_2, \|x_2 - y_2\|_2]. \\ &< \tilde{c}. \end{aligned} \quad (23)$$

Therefore, we have  $[\lambda, x_1, x_2] \in \bar{\Omega}_1$ .

(II) For this goal, we only need to prove

$$\phi([\lambda, x_1, x_2]) \leq c, \text{ for all } \lambda \in [0, 1]. \quad (24)$$

There are three cases to be considered: (i)  $c = 0$ , (ii)  $c < 0$  and (iii)  $c > 0$ . The first case for  $c = 0$  is obvious because  $\Omega_1$  is convex.

(ii) This case is proved via contradiction. Suppose there is a number  $\hat{\lambda} \in [0, 1]$  and a point  $y_{\hat{\lambda}}$  on  $\partial\Omega_1$  such that

$$\|\hat{\lambda}x_1 + (1 - \hat{\lambda})x_2 - y_{\hat{\lambda}}\|_2 = d(\hat{\lambda}) < -c. \quad (25)$$

i.e. the distance between such point and the boundary  $\partial\Omega_1$  is less than  $-c$ . Let's move each point on the section determined by  $x_1, x_2$  parallel with  $d(\hat{\lambda})$  such that  $\mathcal{M}[x_1, x_2, \hat{\lambda}]$  moves to  $y_{\hat{\lambda}}$ , where  $\mathcal{M}$  is defined as follows

$$\mathcal{M}x = x + (y_{\hat{\lambda}} - [x_1, x_2, \hat{\lambda}]). \quad (26)$$

Under the assumption that  $\phi(x_i) = -\min_{y \in \partial\Omega_1} \|x_i - y\| \leq c$ ,  $i = 1, 2$ , i.e. the distances between  $x_i$ ,  $i = 1, 2$ , and  $\partial\Omega_1$  are more than  $-c (> d(\hat{\lambda}))$ . Thus we have  $\mathcal{M}x_1, \mathcal{M}x_2$  are also in the convex set  $\Omega_1$ , so their convex combination  $[\mathcal{M}x_1, \mathcal{M}x_2, \lambda]$  for  $\lambda \in [0, 1]$  is in  $\Omega_1$  as well, which is contradict to  $y_{\hat{\lambda}} = [\mathcal{M}x_1, \mathcal{M}x_2, \hat{\lambda}]$  on  $\partial\Omega_1$ .

(iii) For all  $x_1, x_2 \in \bar{\Omega}_1$  satisfying  $\phi(x_i) \leq c$ , let  $y_i = \arg \min_{y \in \Omega_1} \|x_i - y\|_2$  for  $i = 1, 2$ . Therefore, we have

$$\phi(x_i) \leq \|x_i - y_i\|_2 \leq c, \quad i = 1, 2. \quad (27)$$

Using the same approach for (23), we can get

$$\begin{aligned} \phi([\lambda, x_1, x_2]) &\leq \|[\lambda, x_1, x_2] - [\lambda, y_1, y_2]\|_2 \\ &\leq [\lambda, \|x_1 - y_1\|_2, \|x_2 - y_2\|_2] \leq c. \end{aligned} \quad (28)$$

## Acknowledgement

S. Luo was supported by the Programs for Science and Technology Development of Henan Province (192102310181). X. C. Tai was supported by the startup grant at Hong Kong Baptist University, grants RG(R)-RC/17-18/02-MATH and FRG2/17-18/033. Y. Wang was supported in part by the Hong Kong Research Grant Council grants 16306415 and 16308518. R. Glowinski was supported by the Hong Kong Baptist University and by the Kennedy Wong Foundation.

## References

- [1] Oswin Aichholzer, Franz Aurenhammer, Erik D. Demaine, Ferran Hurtado, Pedro Ramos, and Jorge Urrutia. On  $k$ -convex polygons. *Computational Geometry*, 45(3):73–87, 2012.
- [2] Egil Bae, Xue-Cheng Tai, and Wei Zhu. Augmented Lagrangian method for an Euler’s elastica based segmentation model that promotes convex contours. *Inverse Problems and Imaging*, 11(1):1–23, 2017.
- [3] Vicent Caselles, Ron Kimmel, and Guillermo Sapiro. Geodesic active contours. *International Journal of Computer Vision*, 22(1):61–79, 1997.
- [4] Tony F. Chan and Luminita A. Vese. Active contours without edges. *IEEE Transactions on Image Processing*, 10(2):266–277, 2001.
- [5] Tony F. Chan and Wei Zhu. Level set based shape prior segmentation. In *IEEE Conference on Computer Vision and Pattern Recognition*, volume 2, pages 1164–1170, 2005.
- [6] Virginia Estellers, Dominique Zosso, Rongjie Lai, Stanley Osher, Jean-philippe Thiran, and Xavier Bresson. Method preserving distance function. *IEEE Transactions on Image Processing*, 21(12):4722–4734, 2012.
- [7] Lena Gorelick and Olga Veksler. Multi-object convexity shape prior for segmentation. In *International Workshop on Energy Minimization Methods in Computer Vision and Pattern Recognition*, pages 455–468. Springer, 2017.
- [8] Lena Gorelick, Olga Veksler, Yuri Boykov, and Claudia Nieuwenhuis. Convexity shape prior for binary segmentation. *IEEE Transactions on Pattern Analysis and Machine Intelligence*, 39(2):258–270, 2017.
- [9] Varun Gulshan, Carsten Rother, Antonio Criminisi, Andrew Blake, and Andrew Zisserman. Geodesic star convexity for interactive image segmentation. In *IEEE Conference on Computer Vision and Pattern Recognition*, pages 3129–3136, 2010.
- [10] Hossam Isack, Lena Gorelick, Karin Ng, Olga Veksler, and Yuri Boykov.  $K$ -convexity shape priors for segmentation. In *European Conference on Computer Vision*, pages 36–51, 2018.
- [11] Hossam Isack, Olga Veksler, Milan Sonka, and Yuri Boykov. Hedgehog shape priors for multi-object segmentation. In *IEEE Conference on Computer Vision and Pattern Recognition*, pages 2434–2442, 2016.
- [12] Zili Liu, David W. Jacobs, and Ronen Basri. The role of convexity in perceptual completion: Beyond good continuation. *Vision Research*, 39(25):4244–4257, 1999.
- [13] Shousheng Luo and Xue-Cheng Tai. Convex shape priors for level set representation. *arXiv preprint arXiv:1811.04715*, 2018.
- [14] Rabeeh Karimi Mahabadi, Christian Hane, and Marc Pollefeys. Segment based 3D object shape priors. In *IEEE Conference on Computer Vision and Pattern Recognition*, 2015.
- [15] Pascal Mamassian and Michael S. Landy. Observer biases in the 3D interpretation of line drawings. *Vision Research*, 38(18):2817–2832, 1998.
- [16] David Mumford and Jayant Shah. Optimal approximations by piecewise smooth functions and associated variational problems. *Communications on Pure and Applied Mathematics*, 42(5):577–685, 1989.
- [17] Claudia Nieuwenhuis, Eno Toeppe, Lena Gorelick, Olga Veksler, and Yuri Boykov. Efficient regularization of squared curvature. In *IEEE Conference on Computer Vision and Pattern Recognition*, pages 4098–4105, 2014.
- [18] Mikael Rousson and Nikos Paragios. Shape priors for level set representations. In *European Conference on Computer Vision*, pages 78–92, 2002.
- [19] Loic A. Royer, David L. Richmond, Carsten Rother, Bjoern Andres, and Dagmar Kainmueller. Convexity shape constraints for image segmentation. In *IEEE Conference on Computer Vision and Pattern Recognition*, pages 402–410, 2016.
- [20] James Sethian. A fast marching method for monotonically advancing fronts. In *National Academy of Sciences*, volume 93, pages 1591–1595, 1996.
- [21] Gilbert Strang. The discrete cosine transform. *SIAM Review*, 41(1):135–147, 1999.
- [22] Evgeny Strelakovsky and Daniel Cremers. Generalized ordering constraints for multilabel optimization. In *International Conference on Computer Vision*, pages 2619–2626. IEEE, 2011.
- [23] Fausto A Toranzos and Ana Forte Cunto. Sets expressible as finite unions of star shaped sets. *Journal of Geometry*, 79(1-2):190–195, 2004.
- [24] Yen Hsi Richard Tsai, Li Tien Cheng, Stanley Osher, and Hong Kai Zhao. Fast sweeping algorithms for a class of Hamilton-Jacobi equations. *SIAM Journal on Numerical Analysis*, 41(2):673–694, 2004.
- [25] Eranga Ukwatta, Jing Yuan, Wu Qiu, Martin Rajchl, and Aaron Fenster. Efficient convex optimization-based curvature dependent contour evolution approach for medical image segmentation. In Sebastien Ourselin and David R Haynor, editors, *Medical Imaging 2013: Image Processing*, volume 8669, pages 866–902, 2013.
- [26] Olga Veksler. Star shape prior for graph-cut image segmentation. In *European Conference on Computer Vision*, pages 454–467. Springer, 2008.
- [27] Shi Yan, Xue-Cheng Tai, Jun Liu, and Haiyang Huang. Convexity shape prior for level set based image segmentation method. *arXiv preprint arXiv:1805.08676*, 2018.
- [28] Cong Yang, Xue Shi, Donglan Yao, and Chunming Li. A level set method for convexity preserving segmentation of cardiac left ventricle. In *International Conference on Image Processing*, pages 2159–2163, 2017.
- [29] Sahar Zafari, Tuomas Eerola, Jouni Sampo, Heikki Kälviäinen, and Heikki Haario. Segmentation of partially overlapping convex objects using branch and bound algorithm. In *Asian Conference on Computer Vision*, pages 76–90, 2016.
- [30] Hongkai Zhao. A fast sweeping method for Eikonal equations. *Mathematics of Computation*, 74(250):603–627, 2005.